

# Black carbon and dust alter the response of mountain snow cover under climate change

**Marion REVEILLET** (✉ [marion.reveillet@meteo.fr](mailto:marion.reveillet@meteo.fr))

Univ. Grenoble Alpes, Université de Toulouse, Météo-France, CNRS, CNRM, Centre d'Etudes de la Neige, 38000 Grenoble, France <https://orcid.org/0000-0001-9802-4649>

**Marie Dumont**

Météo-France - CNRS <https://orcid.org/0000-0002-4002-5873>

**Simon Gascoin**

Centre d'Etudes Spatiales de la Biosphère (CESBIO), Université de Toulouse, CNRS/CNES/IRD/INRAE/UPS, 31400 Toulouse, France

**Matthieu Lafaysse**

Univ. Grenoble Alpes, Université de Toulouse, Météo-France, CNRS, CNRM, Centre d'Etudes de la Neige, Grenoble, France

**Pierre Nabat**

CNRM-GAME

**Aurélien Ribes**

Centre National de Recherches Météorologiques <https://orcid.org/0000-0001-5102-7885>

**Rafife Nheili**

Univ. Grenoble Alpes, Université de Toulouse, Météo-France, CNRS, CNRM, Centre d'Etudes de la Neige, 38000 Grenoble, France

**François Tuzet**

Univ. Grenoble Alpes, Université de Toulouse, Météo-France, CNRS, CNRM, Centre d'Etudes de la Neige, Grenoble

**Martin Menegoz**

University of Grenoble

**Samuel Morin**

Univ. Grenoble Alpes, Université de Toulouse, Météo-France, CNRS, CNRM, Centre d'Etudes de la Neige, Grenoble, France <https://orcid.org/0000-0002-1781-687X>

**Ghislain Picard**

Laboratoire de Glaciologie et Géophysique de l'Environnement, CNRS/Université Joseph Fourier de Grenoble

**Paul Ginoux**

National Oceanic and Atmospheric Administration

---

## Article

**Keywords:** snowmelt, water availability, snow cover decline

**Posted Date:** September 9th, 2021

**DOI:** <https://doi.org/10.21203/rs.3.rs-800501/v1>

**License:**   This work is licensed under a Creative Commons Attribution 4.0 International License.

[Read Full License](#)

---

**Version of Record:** A version of this preprint was published at Nature Communications on September 20th, 2022. See the published version at <https://doi.org/10.1038/s41467-022-32501-y>.

# Black carbon and dust alter the response of mountain snow cover under climate change

Marion Réveillet <sup>1\*</sup>, Marie Dumont <sup>1\*</sup>, Simon Gascoin <sup>2</sup>, Matthieu Lafaysse <sup>1</sup>, Pierre Nabat <sup>3</sup>, Aurélien Ribes <sup>3</sup>, Rafife Nheili <sup>1</sup>, Francois Tuzet <sup>1</sup>, Martin Ménégoz <sup>4</sup>, Samuel Morin <sup>3</sup>, Ghislain Picard <sup>4</sup>, Paul Ginoux<sup>5</sup>

<sup>1</sup>Univ. Grenoble Alpes, Université de Toulouse, Météo-France, CNRS, CNRM, Centre d'Etudes de la Neige, 38000 Grenoble, France

<sup>2</sup>Centre d'Etudes Spatiales de la Biosphère (CESBIO), Université de Toulouse, CNRS/CNES/IRD/INRAE/UPS, 31400 Toulouse, France

<sup>3</sup>CNRM, Université de Toulouse, Météo-France, CNRS, Toulouse, France

<sup>4</sup>Univ. Grenoble Alpes, CNRS, IRD, IGE, 38000 Grenoble, France

<sup>5</sup>NOAA Geophysical Fluid Dynamics Laboratory, 201 Forrestal Road, Princeton, NJ 08540, USA

\*To whom correspondence should be addressed; E-mail: marion.reveillet@meteo.fr,  
marie.dumont@meteo.fr

**By darkening the snow surface, mineral dust and black carbon (BC) deposition enhances snowmelt and triggers numerous feedbacks. Assessments of their long-term impact at the regional scale are still largely missing despite the environmental and socio-economic implications of snow cover changes. Here we show, using numerical simulations, that dust and BC deposition has advanced snowmelt by 17 days on average in the French Alps and the Pyrenees over the 1979–2018 period, with major implications for water availability. We demonstrate that the decrease in BC deposition since the 1980s moderates the impact of current warming on snow cover decline. Hence, accounting for changes in light-absorbing particles deposition is required to improve the accuracy of snow cover reanalyses and climate projections, that are crucial for better understanding the past and future evolution of mountain social-ecological systems.**

27 Snow cover changes have drastic consequences for numerous components of the Earth system such as  
28 water resources (1,2), ecosystems (3,4) and the Earth climate through complex feedbacks (5). In response  
29 to climate change, the snow cover duration in mountain areas has declined at the global scale since the  
30 1950s, on average by 5 days per decade at low elevations (6,7). As a response to snow cover decline and  
31 enhanced snowmelt, the peak runoff from snowmelt has shifted by around 10 days on average over the  
32 1965–2005 period for the Alps (8). Changes both in the magnitude and timing of the snowmelt runoff  
33 threaten the availability of water resources in downstream regions, and in particular for irrigation (2).  
34 Snow cover trends are mostly attributed to changes in atmospheric drivers, and especially to the warming  
35 that intensified over the last decades to reach  $0.3\pm 0.2^{\circ}\text{C}$  per decade for mountainous areas at global  
36 scale (6).

37 Light-absorbing particles (LAPs) such as black carbon (BC), brown or organic carbon, mineral dust  
38 and algae are potent drivers of snow cover changes (9–11). LAPs darken the snow surface when deposited  
39 on the snow cover and amplify several snow-albedo feedback loops, drastically modifying the snow cover  
40 evolution and duration (12). LAPs indeed accelerate the coarsening of the snow microstructure, leading to  
41 more solar energy absorption and to an acceleration of the intrinsic snow albedo feedback (13). Moreover,  
42 LAPs are partially retained at the snow surface during melt, amplifying the decrease in the albedo (14).  
43 The impact of LAPs on the snow cover is, thus, modulated by meteorological conditions, leading to  
44 complex interplays between the LAPs and the meteorological drivers of the snow cover evolution (5).

45 BC is the most efficient absorbing aerosol in the atmosphere (12, 15) and its deposition strongly im-  
46 pacts snowmelt rates (12). In central Europe, an increase in BC deposition since 1850 has been observed  
47 until the 1970s due to anthropogenic activities (16). It has been suggested that BC deposition contributed  
48 to the triggering of glacier retreat in the Alps (16). However, BC deposition has decreased since the  
49 1980s (17), due to a reduction of emissions likely related primarily to traffic emission decrease (18).  
50 However, the impact of this recent negative trend on snow cover has not been quantified hitherto.

51 Even if mineral dust deposition events are generally more episodic than BC deposition (19, 20), they  
52 can have a widespread visible impact on the snow surface (e.g. in Feb. 2021, (21)), with a prevailing  
53 radiative effect compared to BC (19, 22). In Europe, mountain ranges are generally affected by dust  
54 deposition events originating from the Sahara, which contribute to 50–70% of the total annual dust de-

55 position (23). Yet, the strong spatial and temporal variability combined with the lack of long-term data  
56 make it difficult to identify trends over the last decades (24).

57 Regional assessments of the combined effect of LAPs deposition on snow cover changes over long  
58 time periods are currently missing (6, 12). Here, we quantify the combined effect of BC and dust deposi-  
59 tion on snow cover dynamic and trends at the regional scale of the French Alps and Pyrenees mountain  
60 ranges, for the 1979–2018 period. Considering the large uncertainty in brown carbon deposition and  
61 absorption efficiency (12), the effect of brown carbon is excluded from the analysis as well as the effect  
62 of algae that generally bloom only at high elevation and late in spring (25). Our analysis is based on  
63 numerical simulations performed with the detailed snow cover model Crocus accounting for the complex  
64 interactions between LAPs and snow (26).

## 65 **Results**

66 Simulations explicitly accounting for dust and BC deposition fluxes are compared to a pure snow sim-  
67 ulation, excluding any LAP. Simulations are driven by the meteorological reanalysis S2M (27) and BC  
68 and dust deposition fluxes from the regional climate model CNRM-ALADIN63 driven by reanalysis data  
69 (so as to follow the unfolding of observed meteorological conditions) (28). To quantify the impact of BC  
70 and dust on snow cover evolution we used the snow melt-out date (SMOD), defined as the last date of  
71 the annual longest period with at least 30 cm of snow. This indicator is relevant for water resources and  
72 ecosystem impacts of the seasonal snow cover (6). The snow cover simulations were evaluated against  
73 satellite observation of the snow cover area and *in situ* observations of melt rates using 495 stations mea-  
74 suring snow depth (See Methods). Simulations accounting for BC and dust systematically lead to better  
75 scores compared to pure snow simulations.

### 76 **Shortening of the season due to BC and dust**

77 The comparison of the pure snow simulations with the simulations accounting for BC and dust show  
78 that, by darkening the snow surface, the combined effect of BC and dust leads to an earlier snow melt-  
79 out date (SMOD) by 17.8 and 16.1 days on average in the French Alps and Pyrenees, respectively, over  
80 the 1979-2018 period (Fig. 1). These reductions correspond to 9.1 and 8.8% of the mean annual snow

81 cover duration. These averages are calculated accounting for the relative surface at each elevation bands  
82 in both mountain ranges. The SMOD reduction varies from 0 to 47 days across the domain (Fig. 1).  
83 Variations depend on the year (Supplementary Fig. S1), due to strong BC and dust variations over time  
84 (Supplementary Fig. S2). Variations also depend on the area and the elevation. A larger absolute impact  
85 of BC and dust on the SMOD in number of days is found at higher elevations. This is related to later melt  
86 and longer snow season, where dust and BC are exposed to higher incoming solar radiation, amplifying  
87 its effect on snowmelt acceleration (29).

88 The effect of BC is prevailing in the Northern part of the French Alps and Pyrenees, where higher BC  
89 deposition is observed (Supplementary Fig. S2). The simulated SMOD when accounting only for BC  
90 is earlier on average by 14.2 days (7.1%) in the Northern Alps and by 13.3 days (6.9%) in the Southern  
91 Alps, compared to the pure simulation. The Southern parts of both mountain ranges are more exposed  
92 to Saharan dust deposition (Supplementary Fig. S2), and exhibit larger dust deposition amounts than  
93 the Northern parts. However the effect of dust deposition is prevailing only at higher elevation in the  
94 Southern parts where the snow cover melts earlier by 3.7 days (1.9%) on average when accounting for  
95 dust only than when accounting for BC only.

96 Figure 1 also shows the SMOD reduction between the pure snow simulation and a simulation named  
97 "baseline" that accounts only implicitly for the LAPs by decreasing albedo as a function of time since  
98 the last snowfall without any link to the actual LAP concentration. This simple treatment of the radiative  
99 impact of LAPs, only represented by a darkening of the surface snow over time, is the most common  
100 practice in snow modeling (30) but has the disadvantage of neglecting spatial or temporal variations of  
101 the LAPs deposition fluxes (see Methods). The simulated SMOD in the baseline configuration is later  
102 compared to the explicit simulation on averaged by 7.3 days for the Alps and 9.3 days for the Pyrenees  
103 (Fig. 1). This suggests that the temporal and spatial variability of the BC and dust deposition fluxes likely  
104 has an important effect on the snow cover duration.

## 105 **BC and dust effect on snow cover inter-annual variability**

106 Based on an analysis of the variance (ANOVA, (31), Method and Supplementary text), we quantify the  
107 contribution of the different atmospheric drivers to the SMOD inter-annual variability (see Methods).  
108 The combined effect of the BC and dust explains up to 30.7% of the variance of the SMOD at 2100 m

109 a.s.l. in the Alps (Fig. 2, total variance of 329 d<sup>2</sup>) and up to 21.8% in the Pyrenees (for a total variance  
110 of 578 d<sup>2</sup>).

111 BC and dust contributions depend on the meteorological conditions (32). For instance, the same  
112 amount of BC and dust deposited at the snow surface has a stronger impact if a large time period between  
113 two snowfalls occurs, than when a snowfall occurs immediately after the deposition. To evaluate this  
114 effect we separate the contribution of the BC and dust only to the total variance (named the additive  
115 part) and the contribution of BC and dust that cannot be separated from the meteorological conditions  
116 (named the sequencing part). This sequencing of meteorological conditions and BC and dust deposition  
117 contributes to 2.9 – 9.1% to the total variance, while the additive part contributes to 12.7 – 25.5% of the  
118 total variance (Fig. 2). These results indicate a marked contribution of BC and dust to the variance of the  
119 SMOD that depends on the meteorological conditions especially in the Southern mountain ranges.

120 The BC and dust contribution to the SMOD inter-annual variability is larger in the Alps than in the  
121 Pyrenees, mostly related to a higher contribution of the BC deposition. BC deposition contributes to 19.3  
122 and 12.4% to the total variance of the SMOD for the Northern and Southern Alps, and to 6.2 and 5.9% for  
123 the Northern and Southern Pyrenees, respectively. BC contribution to the SMOD inter-annual variability  
124 is generally higher than dust contribution, except for the Southern Pyrenees, more affected by episodic  
125 dust outbreaks (33).

126 In summary, our results show that BC and dust are significant drivers of the SMOD inter-annual  
127 variability. The calculation of their contribution has been performed on the 39 years time series without  
128 detrending and thus including the effects of atmospheric trends, such as trends in air temperature and BC  
129 and dust deposition, over this period.

### 130 **Past trends (1979–2018)**

131 The simulated SMOD for pure snow (without considering the BC and dust effect) follows a negative  
132 trend over the last decades (1979–2018) indicating earlier snowmelt (Fig. 3). For instance, the SMOD  
133 decrease at 2100 m a.s.l. is 7.8 days per decade (corresponding to a 4.0% shorter snow season) for the  
134 Northern Alps and 6.4 days per decade (4.0%) for the Southern Alps. This decrease is consistent with  
135 the positive trend in air temperature. According to the reanalysis data used in this study, significant  
136 temperature trends range from 0.1 to 0.3°C per decade (Fig. 3). The SMOD decreasing trend simulated

137 in the Pyrenees is smaller than in the Alps and consistent with the trend in air temperature.

138 The trend in simulated BC deposition over the winter period for the last decades (1979–2018) is  
139 negative (Fig. 3), with a decrease of 11% on average considering all the massifs. Simulations accounting  
140 for BC deposition leads to a negative SMOD trend lower than the SMOD trend of the pure snow case  
141 (Fig. 3). For instance, the SMOD decrease at 2100 m a.s.l. is of 5.2 days per decade for the Northern Alps  
142 (corresponding to a decrease of 2.6% of the snow season duration), 4.0 for the Southern Alps (2.5%). This  
143 means that, at the beginning of the study period (1979–1988), the shortening attributed to BC deposition  
144 alone (i.e. 15 days on average for all the areas) is higher than for the recent period (2009–2018) (i.e. 10  
145 days only in average). Thus, reduced BC deposition fluxes partly offset the effect of rising temperature  
146 because less BC on the snow surface decreases melting rates by reducing solar energy absorption.

147 Conversely, no significant trend in dust deposition is identified (Fig 3). Dust deposition consequently  
148 does not significantly affect the SMOD trend. The decrease in SMOD trend from simulations accounting  
149 for both BC and dust deposition is thus, due to the decrease in BC deposition since the 1980s. This  
150 decrease compensates part of the impact of warming on the trend of the snow cover duration at 2100 m  
151 a.s.l. and is observed for all the Alps and Pyrenees (Supplementary text and Fig. S3) However, trends  
152 presented in this section originate from one model and the limitations are therefore discussed below.

### 153 **Impacts on mountain hydrology**

154 By exerting a strong control on the snow cover ablation rate, BC and dust deposition also has a profound  
155 influence on melt water runoff. To quantify this effect, we use the Center of Mass Date (CMD), defined  
156 as the date for which half of the total annual runoff from snowmelt is reached (34). BC and dust lead to  
157 a shift in the simulated CMD by up to 15 days earlier in the season (Fig. 4) over the 1979-2018 period  
158 compared to pure snow simulations. The effect is larger in the Alps (CMD shift of 15 days for the Alps)  
159 than for the Pyrenees (CMD shift of 10 days) in agreement with the larger effect on snow cover duration  
160 in the Alps mentioned above. No significant change in the intensity of the peak runoff can be attributed  
161 to the presence of BC and dust (Fig. 4). Even if the magnitude of the peak runoff is preserved, earlier  
162 snowmelt can have a profound consequences on the management of the water resource and downstream  
163 alpine ecosystems (35). The combined effect of BC and dust explains up to 5.4 days of the CMD variance  
164 (37% of the total variance, Supplementary Fig. S4). This is in agreement with the contribution of BC

165 and dust found for the SMOD variance with a prevailing contribution of BC deposition on the Northern  
166 ranges and dust deposition in the Southern ranges. The observed changes in the timing of the peak runoff  
167 attributed to climate change over the 1965–2005 period are of around 10 days for the Alps (8). The  
168 simulated CMD shift of 10 to 15 days attributed to the presence of BC and dust here is thus comparable  
169 in magnitude.

170 Finally, our results indicate that the shift of the CMD due to warming would be stronger if not com-  
171 pensated by a decrease in BC deposition over the 1979–2018 period (Fig. 3). When considering only BC  
172 deposition, the trend in CMD would decrease by 1.3 days per decade on average, with a larger impact (of  
173 2 days per decade) in the Northern Alps, explained by a stronger negative trend in BC deposition (Fig.  
174 3).

## 175 **Relevance and implications**

176 This study analyses the impact of dust and BC deposition on seasonal snow cover variability and trends in  
177 the French Alps and Pyrenees, using regional meteorological and deposition reanalysis and the detailed  
178 snow cover model Crocus. We demonstrate that BC and dust have a major role in advancing the snow  
179 cover melt, with a strong influence on the inter-annual variability of the snow cover and drastic implica-  
180 tions for water availability timing. We also show that the response of the snow cover evolution to climate  
181 change is strongly modulated by the BC and dust deposition fluxes, suggesting that trends in snow cover  
182 and LAPs deposition cannot be investigated independently.

183 Our results also show that the impact of BC and dust on SMOD depends strongly on elevation,  
184 in terms of their influence on snowmelt timing (Fig. 1) (29). Indeed when snow is melting later in the  
185 spring (e.g., high elevation) more incoming shortwave energy is available, enhancing the radiative impact  
186 of LAPs. However, these altitudinal variations are superimposed with regional contrasts in the controlling  
187 factors of SMOD changes. The BC and dust deposition leads to larger effect on snow cover duration in  
188 the Alps compared to the Pyrenees directly related to higher BC deposition in the Alps (Supplementary  
189 Fig. S2). The relative impact of dust compared to the one of BC is higher for the South Pyrenees than  
190 for the Alps. This is explained by the regional patterns of African dust deposition that decreases with  
191 the distance to the North African coasts according to a south-north gradient (33) and by the general

192 predominance of African over local sources in the total dust load (36). We can thus expect similarly large  
193 regional contrast in the impact of LAPs on snow cover in other mountainous regions.

194 Strong regional and altitudinal contrasts in BC and dust deposition has also been found for other  
195 mountain ranges as recently evidenced in High Mountain Asia (22). They showed a prevailing of dust  
196 effect on snowmelt at high elevation, especially in the Western regions. The BC and dust load is about  
197 twice higher in these areas than in the Alps and the Pyrenees. The snow cover duration shift induced by  
198 BC and dust in High Mountain Asia is thus likely higher than the 17 days reported in our study for the  
199 French Alps and Pyrenees.

200 Similarly strong regional contrasts arise in the trends of BC and dust deposition. Negative trends  
201 in BC deposition has been observed since the 1980s in Europe but also in North America and in the  
202 Arctic (37, 38). In contrast, positive trends have been reported in Asia, Oceanic regions and Antarctica  
203 (37). Such positive trends may result in enhancing the effect of global warming on snow cover duration.  
204 Regarding dust deposition, no trend is evidenced for most of the mountain regions, partly due to the strong  
205 annual variability of dust deposition and the limited record duration (24). However, a positive trend in  
206 deposition was observed in the Caucasus likely due to increasingly dry conditions in North Africa and  
207 the middle East (39). As exemplified in our study, these regional contrasts in deposition trend modulates  
208 the regional response of the snow cover to climate change.

## 209 **Limitations**

210 Atmospheric and snow cover trends studied here originate from a single land surface mode driven by  
211 a single one meteorological reanalysis (S2M). However, the snow cover trend from our simulations ac-  
212 counting for BC and dust is in line with the observed trends in Alps and Pyrenees (7, 40–42) (see Meth-  
213 ods). Besides, the results of our study are mostly based on relative differences between simulations and  
214 not on absolute values, therefore mitigating the impact of uncertainties in the meteorological variables  
215 and in the surface model. The trend in BC deposition originating from one atmospheric model reported  
216 in this study is in agreement with the negative trend observed in Europe since the 80's, as reported in  
217 many studies (18, 43, 44), and in total conformity with the trend in BC deposition originating from the  
218 atmospheric model GFDL-AM4 (45) (Supplementary Fig. S2).

219 In this study, we considered only two types of LAPs, BC and dust, while other types may also con-  
220 tribute to modify the radiative forcing on the snow cover. Brown carbon was excluded considering the  
221 high uncertainty in atmospheric concentrations and optical properties estimates (12). Snow algae could  
222 play an important contribution to snow cover in some regions such as Greenland (46) but their impact  
223 on seasonal snow in the European Alps is not yet bounded and their impact is limited to the very end of  
224 the snow season and for high elevations (typically above 2000 m a.s.l.) (25, 47). BC and dust are thus  
225 assumed to hold the dominant role in accelerating snow melt. BC and dust optical properties vary consid-  
226 erably (48, 49). The sensitivity to dust refractive index is investigated and the selected index in the study  
227 results in median impact (Supplementary Fig. S5). The sensitivity of our results to this parameter points  
228 out a need to better characterize the optical properties of Saharan dust after long-range transport and  
229 deposition in snow. The absorption efficiency of BC is also prone to large uncertainties (50) especially  
230 in snow (48) and is expected to impact our results. The absorption efficiency chosen here is a moderate  
231 value between extremes found in the literature (32).

232 Bias might also originates from the choice of a scavenging coefficient of BC and dust with melt  
233 water and from the choice of a given snow model. This was quantified using an ensemble approach  
234 with 35 configurations of the snow model showing that the deterministic simulation presented here give  
235 a slightly lower estimate of the impact of BC and dust on SMOD compared to the ensemble simulation  
236 (Supplementary Fig. S6). However, both estimates are close and the temporal trend is conserved. Finally,  
237 BC and dust in the atmosphere may lead to an atmospheric cooling before their deposition on the surface.  
238 Further research would be required to investigate simultaneously the snow cover changes induced by the  
239 deposition and the potential compensating effect of the particles in the atmosphere.

## 240 **Concluding remarks**

241 Our results demonstrate that BC and dust deposition advances the end of the snow season by 17 days  
242 on average over the French Alps and the Pyrenees mountain ranges. This reduction shifts up to 15  
243 days in the availability of water from snowmelt. This has potential environmental and socio-economic  
244 impacts. The BC effect is generally prevailing over the dust effect, especially in the Northern part of the  
245 massifs. BC deposition alone, shortens the snow season by 11 days on average, compared to pure snow

246 simulations. However, the BC effect would be even larger without the decrease in deposition observed  
247 since the 1980s. At the beginning of the study period (1979–1988), a shortening of 15 days is attributed  
248 to BC deposition alone. On the contrary, for the recent period (2009–2018), the shortening due to BC  
249 is of 10 days only on average. This emphasizes the key effect of changes in BC deposition on the snow  
250 cover. Due to the current warming, the snow cover decline would be even more pronounced without the  
251 opposing effect of the decrease in BC deposition since the 1980s. The future changes in BC deposition  
252 related to human activities will therefore be of critical importance for the evolution of the snow cover  
253 in the coming decades. Hence, past and future trends in snow cover and LAPs deposition cannot be  
254 investigated independently. This is crucial to assess the future regional response of mountain hydrology,  
255 water availability, and the future evolution of mountain social-ecological systems.

## 256 **Methods**

### 257 **Site description and atmospheric forcing**

#### 258 **Study sites: French Alps and Pyrenees**

259 The study covers the French Alps and the Pyrenees mountain ranges. In the French Alps, most of the  
260 mountains range between 300 and 3600 m a.s.l. with a maximum at the Mont-Blanc with 4810 m a.s.l..  
261 In this study, the Alps are split into the Northern Alps, with elevation ranging between 1500 to 3000 m  
262 a.s.l. and the Southern Alps with elevation ranging between 1800 to 3000 m a.s.l.. These elevation ranges  
263 are selected as the ones fulfilling the condition of a mean simulated snow depth  $>30$  cm over the winter  
264 period (i.e., 1st of December to 30 of April), and considering all the winters over the 1979–2018 period.  
265 Elevation above 3000 m a.s.l. were excluded because the meteorological forcing and the snow model  
266 Crocus were not thoroughly evaluated in this context (see details below).

267 The Pyrenees mountain range covers distinct mountains located in France, Spain, and Andorra, and  
268 most of them range between 300 and 3000 m a.s.l. with a maximum of 3404 m.a.s.l at the Aneto Peak  
269 (Spain). In this study, the Pyrenees are divided between the Northern and the Southern Pyrenees. The  
270 elevations selected, fulfilling the snow depth condition (i.e., an average larger than 30 cm for the winter  
271 period) are from 1800 to 3000 m a.s.l for the Northern Pyrenees and from 2100 to 3000 m a.s.l. for the  
272 Southern Pyrenees.

## 273 **S2M meteorological reanalysis**

274 The S2M atmospheric reanalysis is built from the SAFRAN (*Système d'Analyse Fournissant des Ren-*  
275 *seignements Atmosphériques à la Neige*) meteorological analysis system (27). SAFRAN data are based  
276 on atmospheric vertical profiles simulated by an atmospheric model (ERA-40 reanalysis until 2001 and  
277 ARPEGE numerical weather prediction model after 2002). These guesses are then corrected by opti-  
278 mal interpolation with mainly observed surface meteorological data from various networks (automatic or  
279 manual observations). SAFRAN do not assimilate any observation above 3000 m a.s.l..

280 SAFRAN outputs include hourly meteorological variables: 2 m air temperature and relative humidity,  
281 precipitation amounts and phases, incoming direct and diffuse shortwave radiation, incoming longwave  
282 radiation, wind speed, cloudiness. These data are assumed to be homogeneous within a given massif.  
283 In SAFRAN geometry, the Alps and the Pyrenees are both divided into 23 massifs defined for their  
284 climatological homogeneity (51). For each massif, meteorological data depends only on elevation (one  
285 data point every 300 m) and and are considered for flat surfaces.

## 286 **BC and dust deposition from CNRM-ALADIN63**

287 BC and dust deposition fluxes are obtained from the regional climate model CNRM-ALADIN63 (28).  
288 This model includes an interactive tropospheric aerosol scheme able to represent the main aerosol species  
289 such as BC and dust in the troposphere. These aerosols are prognostic variables, subject to transport, dry  
290 deposition and in-cloud and below-cloud scavenging. In this study, hourly output of dry and wet BC and  
291 dust deposition fluxes were used, coming from a simulation over the 1979–2018 period driven by the  
292 ERA-Interim reanalysis in order to ensure a realistic timeline of the evolution of aerosol deposition. This  
293 simulations was carried out on a regional domain covering Europe, the Mediterranean Sea and Northern  
294 Africa, at a 12 km horizontal resolution with 91 vertical levels. Data from this simulation have been  
295 chosen as the study performed by (32) indicated a good agreement with the observations at the Col du  
296 Lautaret (Alps, France).

297 Points covering the Alps and Pyrenees are extracted from this simulation, for the period 1979–2018,  
298 and downscaled to obtain BC and dust forcing in SAFRAN geometry. For that purpose, for a given  
299 massif, points located within the massif boundaries were selected. Between 5 to 10 points were selected,

300 depending on the massif area. From these selected points, the hourly mean and the hourly altitudinal  
301 gradient of each variable: dry and wet BC and dust deposition is computed. The hourly gradient is then  
302 applied to the hourly mean to redistribute the data for each 300m steps in agreement with SAFRAN  
303 geometry. Due to differences in precipitation timing between SAFRAN and CNRM-ALADIN63, and  
304 to agree with SAFRAN atmospheric forcing data, hourly dry and wet deposition fluxes are added and  
305 redistributed according to SAFRAN precipitation. Uncertainties of such approach are evaluated (see  
306 Method limitations).

## 307 **Snow cover simulations and evaluation**

### 308 **Simulations description**

309 Simulations are performed with the detailed multilayer snowpack model SURFEX/ISBA-Crocus (52).  
310 Crocus is a detailed snowpack model that includes, among others, dynamical layering, full description  
311 of the surface energy balance, specific surface area, liquid water content as prognostic variable, snow  
312 types, dry and wet snow metamorphism, and an explicit representation of LAPs (the number and types  
313 are users defined) with a fully coupled spectral radiative scheme for solar radiation absorption inside the  
314 snowpack at 20 nm spectral resolution (26). The radiative properties of dust and BC can be user-defined  
315 either based on LAP refractive index or on LAP mass absorption efficiency (26, 32). In the present study,  
316 dust is defined by the mass absorption efficiency from Caponi *et al.* (49) corresponding to dust PM2.5  
317 from Libya in agreement with the study performed by Tuzet *et al.* (32). BC is defined from the constant  
318 refractive index advised by Bond *et al.* (50) (i.e.  $m=1.910.79i$ ). The MAE is then scaled to obtain an  
319 MAE value at 550 nm of  $11.25 \text{ m}^2 \text{ g}^{-1}$  (53). The scaling makes it possible to implicitly account for the  
320 potential absorption enhancement due to internal particle mixing or particle coating.

321 The model ran over the period 1979–2018, in a semi-distributed geometry (i.e., per 300m elevation  
322 bands, for each massif, following the SAFRAN geometry). Contrary to some other applications of the  
323 SAFRAN-Crocus system, we did not extend the simulations to different aspects and slopes. To investigate  
324 the explicit effect of BC and dust on snow cover evolution, four configurations are set up: (i) pure  
325 simulation with no LAP ( $S_{pure}$ ), (ii) simulation considering BC and the dust deposition fluxes ( $S_{BC+Dust}$ ),  
326 (iii) simulation considering BC deposition only ( $S_{BC}$ ) and (iv) a simulation considering dust deposition  
327 only ( $S_{Dust}$ ). Furthermore, the original version of Crocus model (52) considers an implicit representation

328 of LAPs. Indeed, the snow albedo decreases based on the snow age and therefore implicitly considers a  
329 darkening of the snow surface. However this representation is not able to consider temporal variability  
330 of the deposition. For model evaluation, simulations ( $S_{baseline}$ ) performed with this version are compared  
331 to the one allowing an explicit representation of BC and dust (i.e.,  $S_{BC+Dust}$ ).

## 332 **Evaluation**

### 333 1. Using satellite images

334 For each massif, the simulated snow cover area (SCA) and the snow cover duration (SCD) are  
335 compared to the MODIS snow product. MOD10A1 (Terra) and MYD10A1 (Aqua) snow products  
336 are downloaded from the National Snow and Ice Data Center (54, 55) for the period 2000–2016.  
337 The binary snow products are projected on a 500 m resolution grid in the same coordinate system  
338 as the DEM. Missing values, mainly due to cloud obstruction, are interpolated using a stepwise  
339 gapfilling algorithm that was evaluated in the Pyrenees (56). The simulated snow depth is projected  
340 on the same 500 m DEM resolution. Then, a threshold of 0.03 m is used to convert the simulated  
341 snow depth into snow presence or absence for each grid cell (56)). By comparing the simulated and  
342 the observed SCA, results indicate high correlations ( $R^2 > 0.75$ ) and low RMSE (i.e.,  $< 25\%$ ) for all  
343 the simulations. Considering the explicit representation of BC and dust generally leads to a lower  
344 RMSE and a lower bias compared to the other simulations (Supplementary text, Supplementary  
345 Fig. S7).

### 346 2. Comparison with snow depth measurements

347 In order to strengthen the evaluation, simulations are performed at 495 weather station locations  
348 over the French Alps and Pyrenees, covering elevation ranges from 1200 to 2700, over the period  
349 1983–2018. The evaluation is done by comparing the simulated and measured daily snow depth  
350 variations corresponding to melt (57) (Supplementary text). Considering the explicit representation  
351 of BC and dust generally leads to a lower bias compared to the other simulations (Supplementary  
352 Fig. S8).

## 353 Strategy of BC and dust contribution quantification

### 354 1. On the snow cover duration

355 First, the snow melt-out date (SMOD), defined as the last date of the longest period with at least  
356 30cm of snow is computed for each simulation. Then, to quantify the impact of BC and dust on  
357 the shortening of the season, the SMOD differences between  $S_{pure}$  and  $S_{BC+Dust}$  are computed  
358 for each massif, elevations, and years. The differences (i.e.,  $\Delta_{SMOD}$ ) are given by elevation and  
359 locations (Fig. 1), and the spread corresponds to the annual variability. The differences are also  
360 quantified for the simulation between  $S_{pure}$  and  $S_{BC}$  and  $S_{Dust}$  to evaluate the influence of BC and  
361 dust deposition on the snow cover duration separately (Fig. 1) Finally, differences between  $S_{pure}$   
362 and  $S_{baseline}$  are also shown.

### 363 2. On the annual variability of the snow cover

364 A statistical approach based on the variance analysis (ANOVA) is used to evaluate the contri-  
365 bution of the BC and dust on the SMOD annual variability. The detailed method is described in  
366 Geoffroy *et al.* (31) (following the Eq. reported in the Supplementary text). Here, the contribution  
367 of the two parameters "meteorological forcing" and "BC+Dust" to the SMOD variance is computed  
368 (Fig. 2).

### 369 3. On the trend in snow cover

370 The trends in meteorological forcing (temperature and solid precipitation), BC and dust, are com-  
371 puted over the 1979–2018 period, and a Student test (t-test with a 0.05 confidence interval) is  
372 applied to evaluate the significance. The trends in simulated snow cover (SMOD) and CMD of  
373  $S_{pure}$  and  $S_{BC+Dust}$  are quantified following the same method (Fig. 3). Then, for each year, the  
374 SMOD differences between  $S_{pure}$  and  $S_{BC+Dust}$  (and also  $S_{BC}$  and  $S_{Dust}$  separately) is computed,  
375 in order to obtain a dataset (39 years) from these differences. The trend of this dataset is then  
376 computed and its significance is evaluated following the t-test with a 0.05 confidence interval. This  
377 method allows to evaluate the significance of the impact of the BC and dust on the trend.

## 378 **Hydrological impacts**

379 To evaluate the impact of BC and dust on the hydrology, the center of mass date (CMD) of the runoff  
380 from snowmelt is computed for each simulation. The CMD is defined as the date for which 50% of the  
381 total annual runoff from snowmelt is reached (34). The simulated runoff from snowmelt by Crocus is  
382 projected on a 500 m DEM for the Alps and the Pyrenees. The Northern and Southern Alps and the  
383 Pyrenees are considered as four distinct catchments and the total runoff is computed for each catchment  
384 for the 39 years. The mean with the standard deviation (indicating to the temporal variability) is computed  
385 for each catchment considering pure simulations and simulations accounting for BC and dust, to evaluate  
386 the impact of the BC and dust on the runoff amount and timing (Fig. 4). Then, the impact of BC and  
387 dust on the annual variability of the CMD is evaluated following the same method as for the snow cover  
388 described above (Supplementary Fig. S4). The same method as for the snow cover is also applied to  
389 evaluate the impact of the BC and dust on the CMD trends (Fig. 3).

## 390 **Method limitations**

### 391 **Forcing uncertainties**

#### 392 1. Trends

393 As atmospheric and snow cover trends studied here, originate from only one surface model forced  
394 with only one meteorological reanalysis (S2M), comparisons to other models and observations are  
395 required to reinforce our conclusions. All climatological reconstructions are affected by irreducible  
396 uncertainties in the obtained trends due to the temporal heterogeneities of the number and quality of  
397 the data upon which they rely. In particular, Vidal *et al.* (58) demonstrate that the heterogeneities  
398 of available temperature measurements can significantly affect local temperature trends in S2M.  
399 This limitation is expected to be less important when considering large scale signals as in this pa-  
400 per. However, Beaumet *et al.* (59) and Ménégoz *et al.* (60) revealed some large scale differences  
401 in temperature and precipitation trends between S2M analyses and the Regional Climate Model,  
402 MAR, forced by ERA20C reanalysis at the boundaries but not assimilating any observation inside  
403 the simulation domain. Similar discrepancies were obtained in Switzerland by Scherrer and Kot-  
404 larski (61) comparing similar products between S2M and another atmospheric model. However,

405 the snow cover trend from our simulations accounting for BC and dust is in line with the observed  
406 trends. In our simulations, the SMOD trend in the Northern Alps at around 1500 m a.s.l is  $-4.0 \pm 0.6$   
407 days per decade, comparable to the trend observed at Col de Porte ( $-4.1$  days per decade, 1325 m  
408 a.s.l., 1960-2018) (40). In addition, the averaged trend of  $-5.3 \pm 0.6$  days per decade (3.0%) sim-  
409 ulated for the Northern Alps considering elevation ranging between 1500 and 2400 m a.s.l. is in  
410 good agreement with an averaged earlier snowmelt of 5.7 days per decade observed at 11 stations  
411 (covering elevations from 1139 to 2540 m a.s.l) in the Swiss Alps over the 1970–2015 period (41).  
412 In a study based on 202 to 688 stations in the European Alps over the 1971–2019 period, the SCD  
413 computed over the March-May season decreases by  $-7.8$  to  $-0.7\%$  depending on elevation (1000 to  
414 3000 m a.s.l.) and orientation (North or South) (7). The mean relative change of 3.0% from our  
415 simulations is within the range of this study. In the Pyrenees, the absence of significant trend of the  
416 SMOD at 2100 m a.s.l. since 1980 is in agreement with the work of Lopez-Moreno *et al.* (42). Be-  
417 sides, the results of our study are mostly based on relative differences between simulations and not  
418 on absolute value, therefore mitigating the impact of uncertainties in the meteorological variables  
419 and in the surface model.

## 420 2. SAFRAN reanalysis

421 In snow modeling, significant uncertainties are brought by the meteorological forcing (62). Uncer-  
422 tainties in the SAFRAN meteorological reanalysis has been estimated by previous studies (63, 64)  
423 and are highly variable in space. While air temperature biases have not been reported compared  
424 to observations at different locations, radiatif and precipitation biases have been observed. For  
425 instance, Queno *et al.* (57) reported a bias of the shortwave radiation reaching 25 %/ in the Pyre-  
426 nees. Vionnet *et al.* (65) showed an under-estimation of precipitation amount in the Alps at  
427 high elevation. To consider these uncertainties, ensemble methods on the meteorological forcing  
428 are increasingly used. By applying this method, the simulated SMOD uncertainty can reach one  
429 month (66). However, in our study, this impact of this uncertainty is minimized as our conclusions  
430 are based on relative differences between simulations.

## 431 3. BC and dust

432 BC and dust deposition used to force the snowpack model is from only one atmospheric model and

433 could be taken with caution. Still, BC and dust deposition from CNRM-ALADIN63 have been  
434 evaluated by Tuzet et al., (32) at the Col du Lautaret (French Alps) over two snow season. They  
435 showed that compared to the radiative forcing and BC and dust content at the snow surface, sim-  
436 ulated deposition from CNRM-ALADIN63 performs really well ( $R^2=0.78$  between the simulated  
437 and measured absorption and no significant bias are observed between the modeled specific surface  
438 area and the measurements). In addition, annual BC deposition and trend from CNRM-ALADIN63  
439 is in total agreement with BC deposition modeled by GFDL-AM4 (45, 67) (Supplementary Fig.  
440 S2). While dust load from CNRM-ALADIN63 are higher than the one from GFDL-AM4, both  
441 model indicate no significant trend in dust deposition over the period 1980–2014.

442 The BC and dust downscaling method is also prone to uncertainties. Different approaches are  
443 therefore been tested. Firstly, we tested the impact of the number of points selected in each mas-  
444 sif with and without considering a weight depending on the point location using the downscaling  
445 methodology. Results do not lead to significant differences in total BC and dust deposition (differ-  
446 ences lower than 5% ) when computing this deposition with a different number of points selected  
447 for a given massif. Second, another method to compute the altitudinal gradient, used to redistribute  
448 the BC and dust deposition, is tested. This gradient is computed using the concentration profiles  
449 of the BC and dust in the atmosphere instead of the BC and dust deposition. With the hypothesis  
450 that the atmospheric profile is conserved for the altitudinal variation of the deposition, the monthly  
451 gradient is computed from the monthly data of the BC and dust concentration profile available. In  
452 this case, dry and wet deposition cannot be separated and the gradient is relatively homogeneous  
453 for all the locations. The maximum difference in BC and dust deposition between the two methods  
454 is 30% for the BC and 45% for the dust deposition. This method hasn't been chosen due to the  
455 unrealistic homogeneous gradient obtained. Finally, the dry and wet distribution method following  
456 the SAFRAN precipitation events can be questionable. A sensitivity test by performing a simu-  
457 lation considering all the fluxes as dry deposition indicated a mean difference lower than one day  
458 (with a maximum of 4 days observed at highest elevations) compared to the simulation performed  
459 with the method described in this study. Larger differences are observed when considering all the  
460 fluxes as wet deposition where a maximum of -15 days is observed at the highest elevation with a

461 mean of 4 days. Yet, this uncertainty is lower than the SMOD differences calculated related to the  
462 effect of BC and dust on the snow cover duration.

## 463 **Model uncertainties**

### 464 1. Optical properties of BC and dust

465 The choice of dust refractive index and mass absorption coefficients also implies some uncertain-  
466 ties. In this study, value for Saharan Libya PM2-5 (49) are chosen: a mass absorption efficiency at  
467 400 nm of  $110 \cdot 10^{-3} \text{ m}^2 \text{ g}^{-1}$  and a dust Angstrom exponent equal to 4.1. This choice was made as  
468 Saharan dust is the primary source of dust deposition in European mountainous areas and as Tuzet  
469 *et al.* (32) demonstrated based on spectral reflectance measurements that this spectral signature  
470 agrees well with the measured spectrum for two winter seasons. However, this spectral signature  
471 is expected to vary significantly with the source location which varies over time. Simulations per-  
472 formed by changing this spectral signature, with a mass absorption efficiency at 400nm ranging  
473 between  $27 \cdot 10^{-3} \text{ m}^2 \text{ g}^{-1}$  (corresponding to the source Sahel – Bodélé PM10) and  $630 \cdot 10^{-3} \text{ m}^2$   
474  $\text{g}^{-1}$  (for dust PM2-5 from Sahel – Mali). The Angstrom exponent is equal to 3.3 (Bodélé) and 3.4  
475 (Mali). This sensitivity study allows quantifying the uncertainty related to the spectral signature  
476 chosen (Supplementary Fig. S5). Depending on this calibration, the median of the  $\Delta\text{SMOD}$  at  
477 2100 m a.s.l. vary between 15 to 25 and 12 to 23 for the North and South Alps respectively, and  
478 between 11 to 20 and 10 to 21 for the North and South Pyrenees respectively. The median of the  
479  $\Delta\text{SMOD}$  with the spectral signature chosen in this study is closer to the lower median (i.e. 19  
480 (15) for the North (South) Alps and 13 for both the North and South Pyrenees), suggesting that the  
481 effect of dust reported in this study might be under-estimated, especially for Saharan event from lo-  
482 cation close to Mali. Finally, additional uncertainties are also associated with the modelling of BC  
483 absorption efficiency in snow. Indeed, the evolution of this parameter are still poorly understood  
484 with variations of at least a factor 2 reported in the literature (e.g. Tuzet *et al.* (48) and references  
485 therein).

### 486 2. Scavenging of BC and dust

487 In this study the scavenging of impurities in the snowpack was not considered (32). Indeed, the lack

488 of quantitative observations of LAPs percolation at the snow surface in presence of melt water does  
489 not allow a proper evaluation of this effect. Moreover, Crocus percolation schemes are quite simple  
490 and are expected to be entached with many uncertainties. A sensitivity test has nevertheless been  
491 performed, allowing 20% of the BC (5% of the dust) to scavenged with the water percolation (26).  
492 This leads to a negligible effect (i.e. a median of the  $\Delta$ SMOD variation at 2100 m a.s.l. of 2 days  
493 for the North Alps and 1 day for the South Alps).

### 494 3. Representation in snow physics

495 Large uncertainties remain also in the representation of the snow physics, and Skiles and Painter  
496 (68) quantified a SMOD difference around 30 days depending on the complexity of the snow model  
497 chosen (degree-day snow model vs detailed snow model). Using an ensemble approach considering  
498 35 different state-of-the art parameterisations in Crocus, Dumont *et al.* (29) indicates a SMOD  
499 variation around 5 days, highlighting the uncertainty related to the selected snow physic in the  
500 model. In this study, we quantified the model uncertainty using an ensemble approach considering  
501 35 different state-of-the art parameterisations in Crocus (69) to simulate the delta SMOD at 2100  
502 m a.s.l. (Supplementary Fig. S6). Uncertainties related to model physic choice and location (i.e.  
503 box plot size of the ensemble simulations) is within the same range than the location uncertainty  
504 (i.e. the box plot size of the deterministic simulation in Supplementary Fig. S6).

### 505 4. Geometry of the simulations

506 Simulations are performed in a semi-distributed geometry only considering a flat aspect. This is  
507 because the slope and aspect represent a huge amount of additional data, complex to be considered  
508 in the simulations. Still, with a simulation considering the slope and aspect, we expect a higher  
509 impact of the BC and dust deposition on the snowpack evolution for southern slopes compared  
510 to flat areas (and the opposite for the Northern slopes). Southern slopes are indeed exposed to  
511 considerably higher solar radiation.

## 512 **References**

- 513 1. Barnett, T. P., Adam, J. C. & Lettenmaier, D. P. Potential impacts of a warming climate on water  
514 availability in snow-dominated regions. *Nature* **438**, 303–309 (2005).
- 515 2. Mankin, J. S. & Diffenbaugh, N. S. Influence of temperature and precipitation variability on near-term  
516 snow trends. *Climate Dynamics* **45**, 1099–1116 (2015).
- 517 3. Ernakovich, J. G. *et al.* Predicted responses of arctic and alpine ecosystems to altered seasonality  
518 under climate change. *Global Change Biology* **20**, 3256–3269 (2014).
- 519 4. Hoegh-Guldberg, O. *et al.* Impacts of 1.5 c global warming on natural and human systems. *Global*  
520 *warming of 1.5 C. An IPCC Special Report* (2018).
- 521 5. Flanner, M. G., Shell, K. M., Barlage, M., Perovich, D. K. & Tschudi, M. Radiative forcing and albedo  
522 feedback from the northern hemisphere cryosphere between 1979 and 2008. *Nature Geoscience* **4**,  
523 151–155 (2011).
- 524 6. Hock, R. *et al.* High mountain areas: Ipcc special report on the ocean and cryosphere in a changing  
525 climate (2019).
- 526 7. Matiu, M. *et al.* Observed snow depth trends in the european alps: 1971 to 2019. *The Cryosphere* **15**,  
527 1343–1382 (2021).
- 528 8. Hartmann, D. *et al.* *Observations: Atmosphere and Surface*, book section 2, 159–254 (Cam-  
529 bridge University Press, Cambridge, United Kingdom and New York, NY, USA, 2013). URL  
530 [www.climatechange2013.org](http://www.climatechange2013.org).
- 531 9. Wiscombe, W. J. & Warren, S. G. A model for the spectral albedo of snow. i: Pure snow. *Journal of*  
532 *Atmospheric Sciences* **37**, 2712–2733 (1980).
- 533 10. Painter, T. H., Skiles, S. M., Deems, J. S., Brandt, W. T. & Dozier, J. Variation in rising limb of  
534 colorado river snowmelt runoff hydrograph controlled by dust radiative forcing in snow. *Geophysical*  
535 *Research Letters* **45**, 797–808 (2018).

- 536 11. Warren, S. G. Light-absorbing impurities in snow: a personal and historical account. *Frontiers in*  
537 *Earth Science* **6**, 250 (2019).
- 538 12. Skiles, S. M., Flanner, M., Cook, J. M., Dumont, M. & Painter, T. H. Radiative forcing by light-  
539 absorbing particles in snow. *Nature Climate Change* **8**, 964–971 (2018).
- 540 13. Dumont, M. *et al.* Contribution of light-absorbing impurities in snow to greenland’s darkening since  
541 2009. *Nature Geoscience* **7**, 509–512 (2014).
- 542 14. Sterle, K. M., McConnell, J. R., Dozier, J., Edwards, R. & Flanner, M. G. Retention and radiative  
543 forcing of black carbon in eastern sierra nevada snow. *The Cryosphere* **7**, 365–374 (2013). URL  
544 <https://tc.copernicus.org/articles/7/365/2013/>.
- 545 15. Flanner, M. G., Zender, C. S., Randerson, J. T. & Rasch, P. J. Present-day climate forcing and  
546 response from black carbon in snow. *Journal of Geophysical Research: Atmospheres* **112** (2007).
- 547 16. Painter, T. H. *et al.* End of the little ice age in the alps forced by industrial black carbon. *Proceedings*  
548 *of the national academy of sciences* **110**, 15216–15221 (2013).
- 549 17. Lim, S. *et al.* Black carbon variability since preindustrial times in the eastern part of europe recon-  
550 structed from mt. elbrus, caucasus, ice cores. *Atmospheric Chemistry and Physics* **17** (2017).
- 551 18. Kutzner, R. D. *et al.* Long-term monitoring of black carbon across germany. *Atmospheric Environ-*  
552 *ment* **185**, 41–52 (2018).
- 553 19. Kaspari, S., Painter, T. H., Gysel, M., Skiles, S. & Schwikowski, M. Seasonal and elevational  
554 variations of black carbon and dust in snow and ice in the solu-khumbu, nepal and estimated radiative  
555 forcings. *Atmospheric Chemistry and Physics* **14**, 8089–8103 (2014).
- 556 20. Di Mauro, B. *et al.* Mineral dust impact on snow radiative properties in the european alps combining  
557 ground, uav, and satellite observations. *Journal of Geophysical Research: Atmospheres* **120**, 6080–  
558 6097 (2015).
- 559 21. Réveillet, M. *et al.* Dépôts massifs de poussières sahariennes sur le manteau neigeux dans les Alpes  
560 et les Pyrénées du 5 au 7 février 2021 : Contexte, enjeux et résultats préliminaires Version du 3

- 561 mai 2021. Technical Report, CNRM, Université de Toulouse, Météo-France, CNRS (2021). URL  
562 <https://hal.archives-ouvertes.fr/hal-03216273>.
- 563 22. Sarangi, C. *et al.* Dust dominates high-altitude snow darkening and melt over high-mountain asia.  
564 *Nature Climate Change* **10**, 1045–1051.
- 565 23. Ginoux, P. *et al.* Sources and distributions of dust aerosols simulated with the gocart model. *Journal*  
566 *of Geophysical Research: Atmospheres* **106**, 20255–20273 (2001).
- 567 24. Chedin, A., Capelle, V. & Scott, N. Detection of iasi dust aod trends over sahara: How many years  
568 of data required? *Atmospheric Research* **212**, 120–129 (2018).
- 569 25. Di Mauro, B., Garzonio, R. & Baccolo, G. e. a. Glacier algae foster ice-albedo feedback in the  
570 european alps. *Scientific Reports* **10** (2020).
- 571 26. Tuzet, F. *et al.* A multilayer physically based snowpack model simulating direct and indirect radiative  
572 impacts of light-absorbing impurities in snow. *The Cryosphere* **11** (2017).
- 573 27. Vernay, M. *et al.* The S2M meteorological and snow cover reanalysis in the French mountainous  
574 areas (1958–present), Data set, AERIS (2019).
- 575 28. Nabat, P. *et al.* Modulation of radiative aerosols effects by atmospheric circulation over the  
576 euro-mediterranean region. *Atmospheric Chemistry and Physics* **20**, 8315–8349 (2020). URL  
577 <https://acp.copernicus.org/articles/20/8315/2020/>.
- 578 29. Dumont, M. *et al.* Accelerated snow melt in the Russian Caucasus mountains after the Saharan dust  
579 outbreak in March 2018. *Journal of Geophysical Research: Earth Surface* **125** (2020).
- 580 30. Essery, R., Morin, S., Lejeune, Y. & Ménard, C. B. A comparison of 1701 snow models using  
581 observations from an alpine site. *Advances in Water Resources* **55**, 131–148 (2013).
- 582 31. Geoffroy, O., Saint-Martin, D. & Ribes, A. Quantifying the sources of spread in climate change  
583 experiments. *Geophysical Research Letters* **39** (2012).

- 584 32. Tuzet, F. *et al.* Quantification of the radiative impact of light-absorbing particles during two con-  
585 trasted snow seasons at col du lautaret (2058 m asl, french alps). *The Cryosphere Discussions* 1–38  
586 (2020).
- 587 33. Vincent, J. *et al.* Variability of mineral dust deposition in the western mediterranean basin and  
588 south-east of france (2016).
- 589 34. McCabe, G. J. & Clark, M. P. Trends and variability in snowmelt runoff in the western united states.  
590 *Journal of Hydrometeorology* **6**, 476–482 (2005).
- 591 35. Bard, A. *et al.* Trends in the hydrologic regime of alpine rivers. *Journal of Hydrology* **529**, 1823–  
592 1837 (2015).
- 593 36. Pey, J. *et al.* Snow impurities in the central pyrenees: From their geochemical and mineralogical  
594 composition towards their impacts on snow albedo. *Atmosphere* **11**, 937 (2020).
- 595 37. Ningombam, S. S. *et al.* Long-term (1995–2018) aerosol optical depth derived using ground based  
596 aernet and skynet measurements from aerosol aged-background sites. *Atmospheric Pollution Re-*  
597 *search* **10**, 608–620 (2019).
- 598 38. Sharma, S. *et al.* Widespread loss of lake ice around the northern hemisphere in a warming world.  
599 *Nature Climate Change* **9**, 227–231 (2019).
- 600 39. Kutuzov, S. *et al.* The elbrus (caucasus, russia) ice core record–part 2: history of desert dust deposi-  
601 tion. *Atmospheric Chemistry and Physics* **19** (2019).
- 602 40. Lejeune, Y. *et al.* 57 years (1960–2017) of snow and meteorological observations from a mid-altitude  
603 mountain site (col de porte, france, 1325 m of altitude). *Earth System Science Data* **11**, 71–88 (2019).  
604 URL <https://essd.copernicus.org/articles/11/71/2019/>.
- 605 41. Klein, G., Vitasse, Y., Rixen, C., Marty, C. & Rebetez, M. Shorter snow cover duration since 1970 in  
606 the swiss alps due to earlier snowmelt more than to later snow onset. *Climatic Change* **139**, 637–649  
607 (2016).

- 608 42. López-Moreno, J. *et al.* Long-term trends (1958–2017) in snow cover duration and depth in the  
609 pyrenees. *International Journal of Climatology* (2020).
- 610 43. Sun, J. *et al.* Decreasing trends of particle number and black carbon mass concentrations at 16  
611 observational sites in germany from 2009 to 2018. *Atmospheric Chemistry and Physics* **20**, 7049–  
612 7068 (2020).
- 613 44. Grange, S. K., Lötscher, H., Fischer, A., Emmenegger, L. & Hueglin, C. Evaluation of equivalent  
614 black carbon source apportionment using observations from switzerland between 2008 and 2018.  
615 *Atmospheric Measurement Techniques* **13** (2020).
- 616 45. Zhao, M. *et al.* The gfdl global atmosphere and land model am4. 0/m4. 0: 1. simulation character-  
617 istics with prescribed ssts. *Journal of Advances in Modeling Earth Systems* **10**, 691–734 (2018).
- 618 46. Hoham, R. W. & Remias, D. Snow and glacial algae: A review1. *Journal of phycology* **56**, 264–282  
619 (2020).
- 620 47. Stewart, A. *et al.* Altitudinal zonation of green algae biodiversity in the french alps. *Frontiers in*  
621 *Plant Science* **12**, 1066 (2021).
- 622 48. Tuzet, F. *et al.* Influence of light-absorbing particles on snow spectral irradiance profiles. *The*  
623 *Cryosphere* **13**, 2169–2187 (2019).
- 624 49. Caponi, L. *et al.* Spectral-and size-resolved mass absorption efficiency of mineral dust aerosols in the  
625 shortwave spectrum: a simulation chamber study. *Atmospheric Chemistry and Physics* **17**, 7175–7191  
626 (2017).
- 627 50. Bond, T. C. & Bergstrom, R. W. Light absorption by carbonaceous particles: An investigative review.  
628 *Aerosol science and technology* **40**, 27–67 (2006).
- 629 51. Durand, Y. *et al.* Reanalysis of 44 yr of climate in the french alps (1958–2002): methodology,  
630 model validation, climatology, and trends for air temperature and precipitation. *Journal of Applied*  
631 *Meteorology and Climatology* **48**, 429–449 (2009).

- 632 52. Vionnet, V. *et al.* The detailed snowpack scheme crocus and its implementation in surfex v7. 2  
633 (2012).
- 634 53. Hadley, O. L. & Kirchstetter, T. W. Black-carbon reduction of snow albedo. *Nature Climate Change*  
635 **2**, 437–440 (2012).
- 636 54. Hall, D. K., Riggs, G. A. & Salomonson, V. V. Modis snow and sea ice products. *Earth science*  
637 *satellite remote sensing* 154–181 (2006).
- 638 55. Hall, D. K. & Riggs, G. A. Accuracy assessment of the modis snow products. *Hydrological Pro-*  
639 *cesses: An International Journal* **21**, 1534–1547 (2007).
- 640 56. Gascoïn, S. *et al.* A snow cover climatology for the pyrenees from modis snow products (2015).
- 641 57. Quéno, L., Karbou, F., Vionnet, V. & Dombrowski-Etchevers, I. Satellite products of incoming solar  
642 and longwave radiations used for snowpack modelling in mountainous terrain. *Hydrology and Earth*  
643 *System Sciences Discussions* 1–33 (2017).
- 644 58. Vidal, J. P., Martin, E., Franchistéguy, L., Baillon, M. & Soubeyroux, J.-M. A 50-year high-  
645 resolution atmospheric reanalysis over france with the safran system. *International Journal of Clima-*  
646 *tology* **30**, 1627–1644 (2010).
- 647 59. Beaumet, J. *et al.* Twentieth century temperature and snow cover changes in the french alps using  
648 a high-resolution regional climate model and reanalyses. *Regional Environmental Change* (under  
649 review).
- 650 60. Ménégoz, M. *et al.* Contrasting seasonal changes in total and intense precipitation in the european  
651 alps from 1903 to 2010. *Hydrology and Earth System Sciences Discussions* 1–37 (2020).
- 652 61. Scherrer, S. C. Temperature monitoring in mountain regions using reanalyses: Lessons from the  
653 alps. *Environmental Research Letters* **15**, 044005 (2020).
- 654 62. Raleigh, M., Lundquist, J. & Clark, M. Exploring the impact of forcing error characteristics on  
655 physically based snow simulations within a global sensitivity analysis framework. *Hydrology & Earth*  
656 *System Sciences* **19** (2015).

- 657 63. Quintana-Segui, P. *et al.* Analysis of near-surface atmospheric variables: Validation of the safran  
658 analysis over france. *Journal of applied meteorology and climatology* **47**, 92–107 (2008).
- 659 64. Charrois, L. *et al.* On the assimilation of optical reflectances and snow depth observations into a  
660 detailed snowpack model (2016).
- 661 65. Vionnet, V. *et al.* Sub-kilometer precipitation datasets for snowpack and glacier modeling in alpine  
662 terrain. *Frontiers in Earth Science* **7**, 182 (2019).
- 663 66. Cluzet, B. *et al.* Croco\_v1. 0: a particle filter to assimilate snowpack observations in a spatialised  
664 framework. *Geoscientific Model Development Discussions* 1–36 (2020).
- 665 67. Zhao, M. *et al.* The gfdl global atmosphere and land model am4. 0/lm4. 0: 2. model description,  
666 sensitivity studies, and tuning strategies. *Journal of Advances in Modeling Earth Systems* **10**, 735–769  
667 (2018).
- 668 68. Skiles, S. M. & Painter, T. H. Toward understanding direct absorption and grain  
669 size feedbacks by dust radiative forcing in snow with coupled snow physical and ra-  
670 diative transfer modeling. *Water Resources Research* **55**, 7362–7378 (2019). URL  
671 <https://agupubs.onlinelibrary.wiley.com/doi/abs/10.1029/2018WR024573>.  
672 <https://agupubs.onlinelibrary.wiley.com/doi/pdf/10.1029/2018WR024573>.
- 673 69. Lafaysse, M. *et al.* A multiphysical ensemble system of numerical snow modelling. *The Cryosphere*  
674 **11**, 1173–1198 (2017).

675 **Acknowledgements.** The authors thank Florent Dominé and Delphine Six for helpful conversations.

676

677 **Funding.** CNRM/CEN and IGE are part of Labex OSUG@2020 (investissement d’avenir - ANR10  
678 LABX56). This study was supported by the ANR program ANR-16-CE01-0006 EBONI; the INSU/LEFE  
679 project ASSURANCE, and the CNES APR grant MIOSOTIS. This research was at least partially sup-  
680 ported by Lautaret Garden-UMS 3370 (Univ.Grenoble Alpes, CNRS, SAJF, 38000 Grenoble, France),  
681 member of AnaEE-France (ANR-11-INBS-0001AnaEE-Services, Investissements d’Avenir frame) and

682 of the eLTER-Europe network (Univ. Grenoble Alpes, CNRS, LTSER Zone Atelier Alpes, 38000 Greno-  
683 ble, France). As part of the project CDP TRAJECTORIES, M. M. has been funded by the French National  
684 Research Agency in the framework of the “Investissements d’avenir” programme (ANR-15-IDEX-02).

685

686 **Author Contributions.** M. R. led the study and performed the simulations and analysis. M.D. designed  
687 the study. M.R. and M.D. wrote the paper with contributions from all co-authors. S.G. provided the  
688 MODIS data and contributed to the analysis. F.T., M.L. and R.N. implemented the Crocus version with  
689 explicit representation of LAPs. P.N. and P.G. provided atmospheric simulations including LAPs deposi-  
690 tion and contributed to the analysis. A.R. contributed the ANOVA and trends computations and analysis.  
691 M.M. contributed to the downscaling method for the LAPs fluxes and to the analysis.

692

693 **Competing Interests.** The authors declare that they have no competing interests.

694

695 **Data and code availability.** The dataset will be published on an open-access platform (with a DOI) after  
696 the review process. While it is not yet implemented in an official SURFEX release, the code will be  
697 downloadable from a specific tag of the git repository maintained by Centre d’Études de la Neige upon  
698 publication of the paper. The full procedure and documentation to access this git repository can be found  
699 at : [https://opensource.cnrm-game-meteo.fr/projects/snowtools\\_git/wiki](https://opensource.cnrm-game-meteo.fr/projects/snowtools_git/wiki). Tartes model is available here:  
700 <http://snowtartes.pythonanywhere.com/> (web application and Python module download).

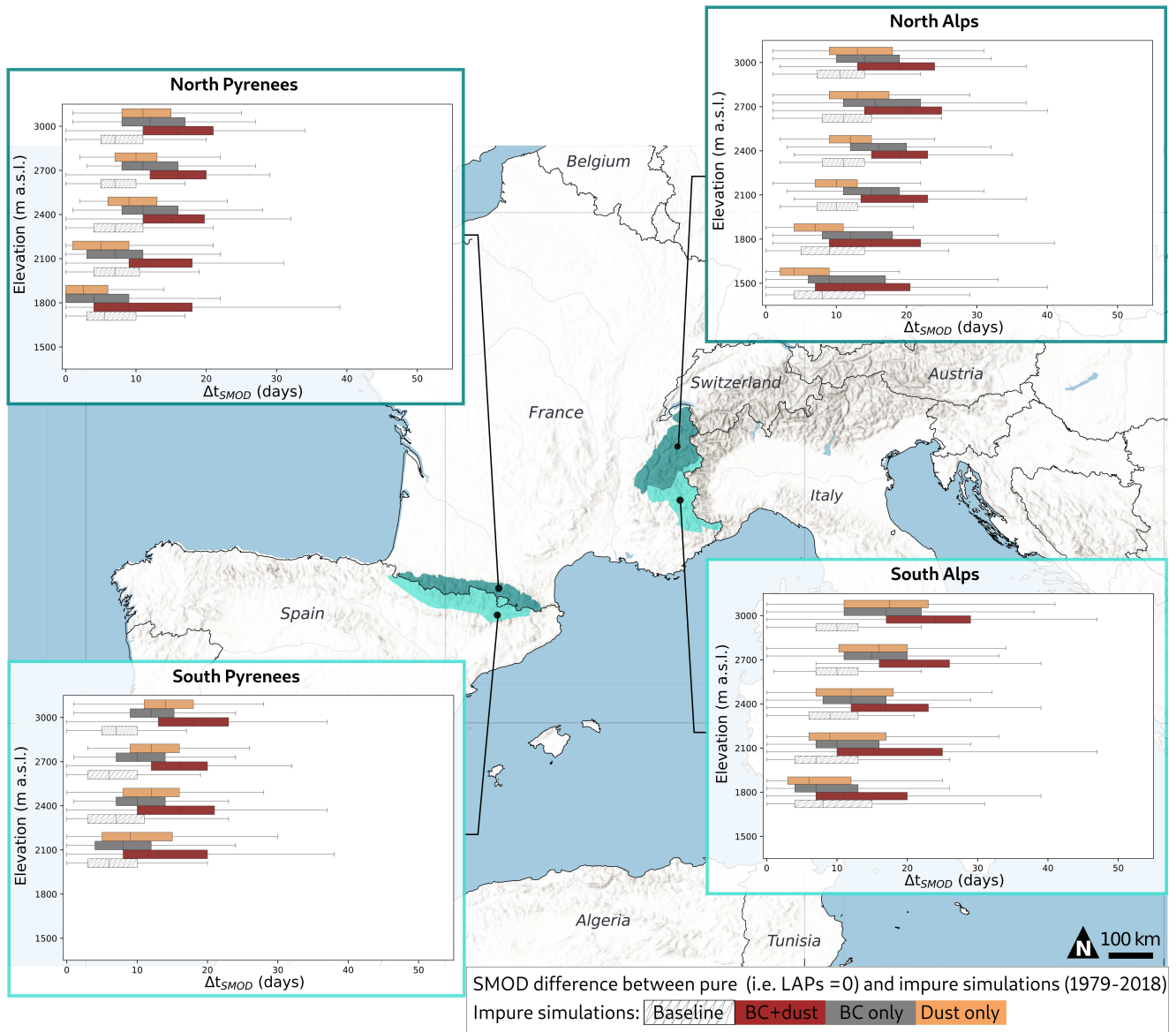


**Fig. 1: Shortening of the snow season related to BC and dust deposition** This shortening is computed as the difference in snow melt-out date (SMOD) between the pure snow simulations and all the configurations: simulations considering BC and dust (brown), only BC (grey), only dust (orange), considering implicitly the LAPs (i.e. an albedo decrease based on the snow age only, green). SMOD differences are computed as a function of the elevation, computed considering the entire study period (i.e., 1978–2018), for the North and South Pyrenees (left) and the North and South Alps (right). The boxes show the quartiles of the distribution corresponding to the inter-annual and spatial variability. Minimum/maximum ranges (excluding outliers) are indicated by the whiskers. Only elevations with a mean SD >30 cm over the winter period (i.e. 1st of December to 30 of April) are represented.

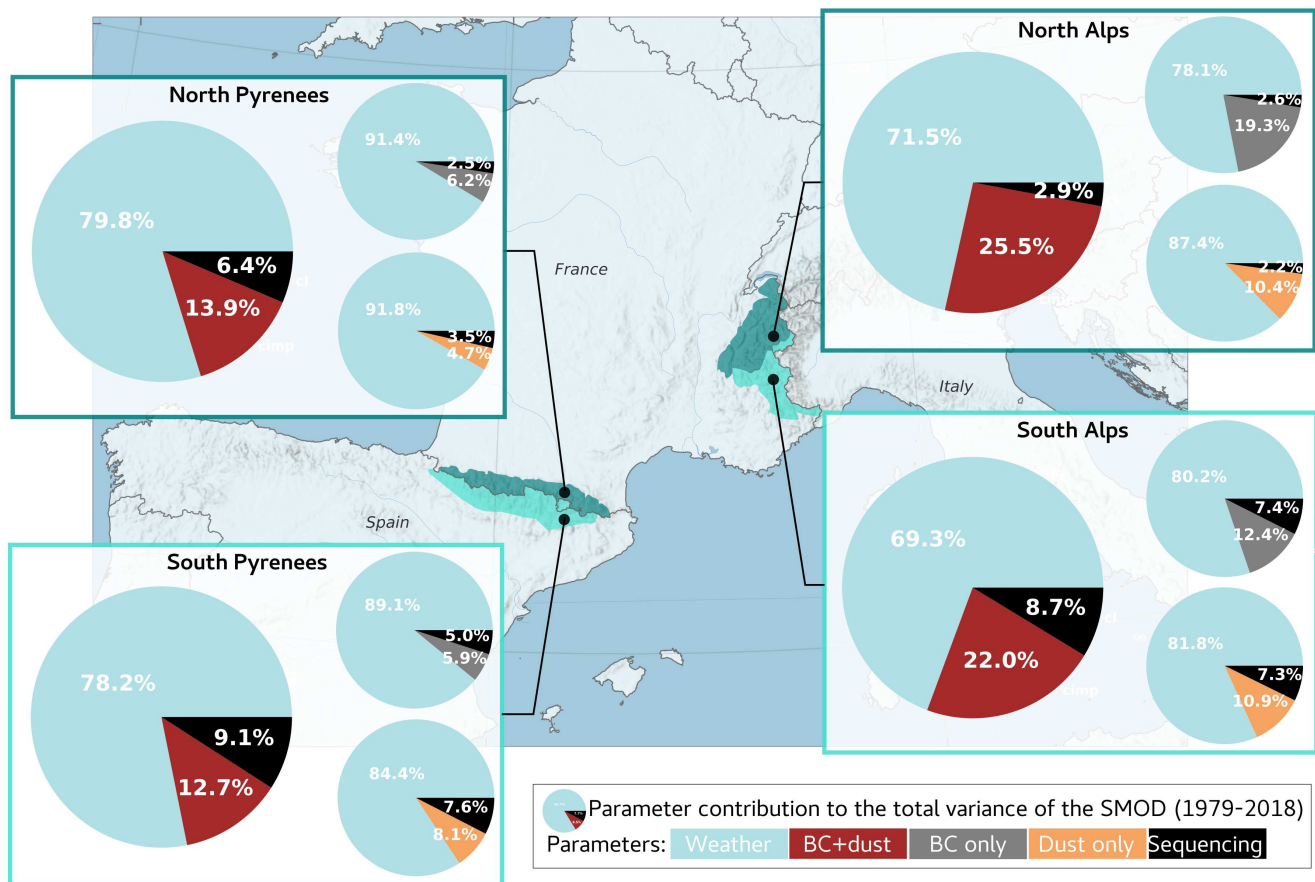


**Fig. 2: Contribution of the meteorological conditions and BC and dust to the variance of the SMOD.** Contributions computed over the 1979–2018 period at 2100 m a.s.l. for the North and South Pyrenees (left), North and South Alps (right). Larger circles indicate contributions of the parameters considering the role of BC+Dust (brown) and smaller circles represent the contribution of BC (grey) and dust (orange) separately. The sequencing term (black) indicates the contribution of BC and dust and meteorological forcing, and is due to the dependence of the BC and dust contribution to the meteorological conditions.

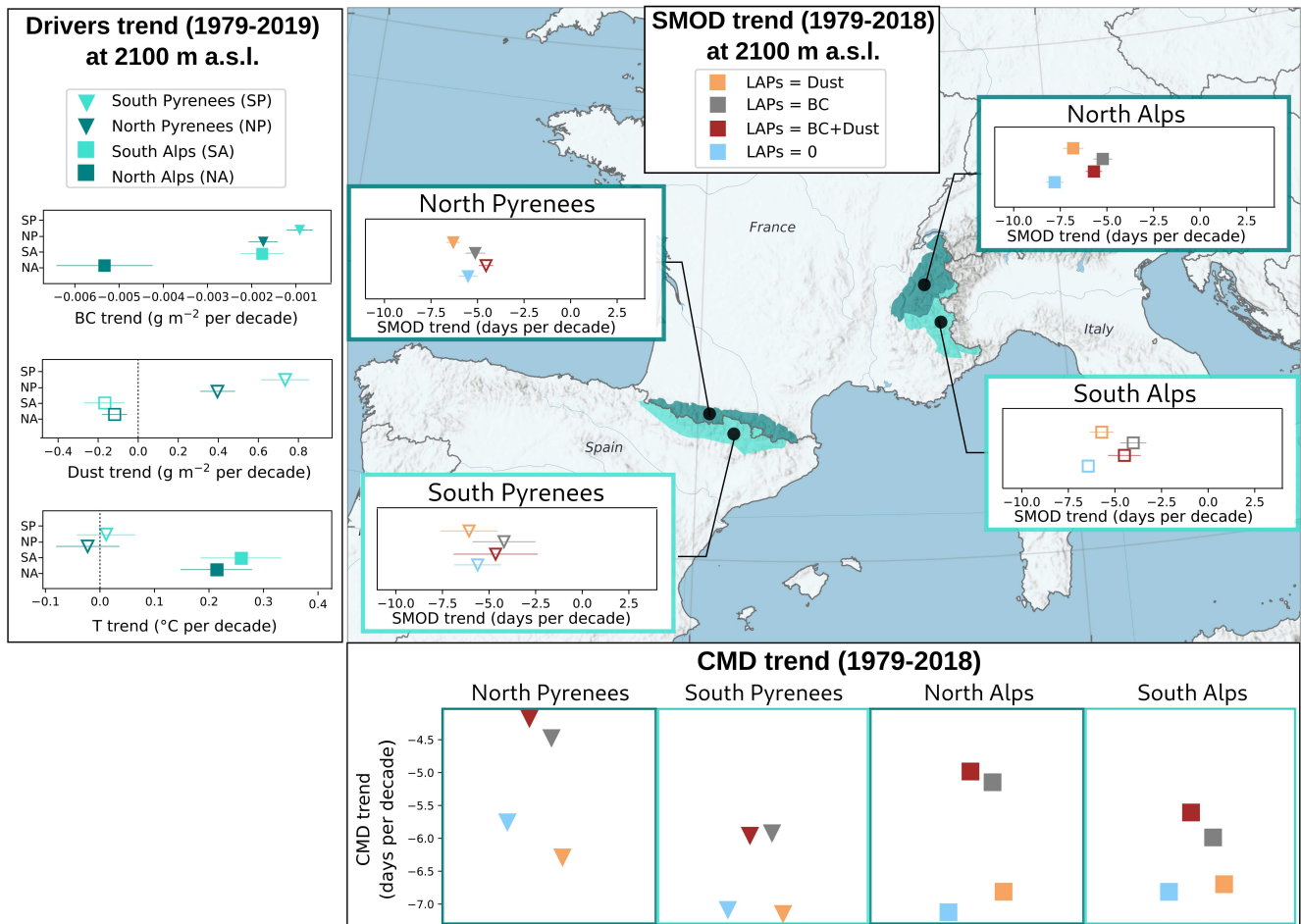


**Fig. 3: Trends in air temperature (at 2m above the surface), BC and dust deposition, SMOD and center of mass date (CMD) over 1979–2018.** Trends are from temporal series computed from annual values at 2100 m a.s.l.. Trends are represented as the the best estimate and 90% confidence range, per area (North Alps, South Alps, North Pyrenees and South Pyrenees). Only markers of significant trends (t-test 0.05) are filled in. Error bars represent the spatial variability. Only elevations with a mean SD >30 cm over the winter period (i.e. 1st of December to 30 of April) are represented.

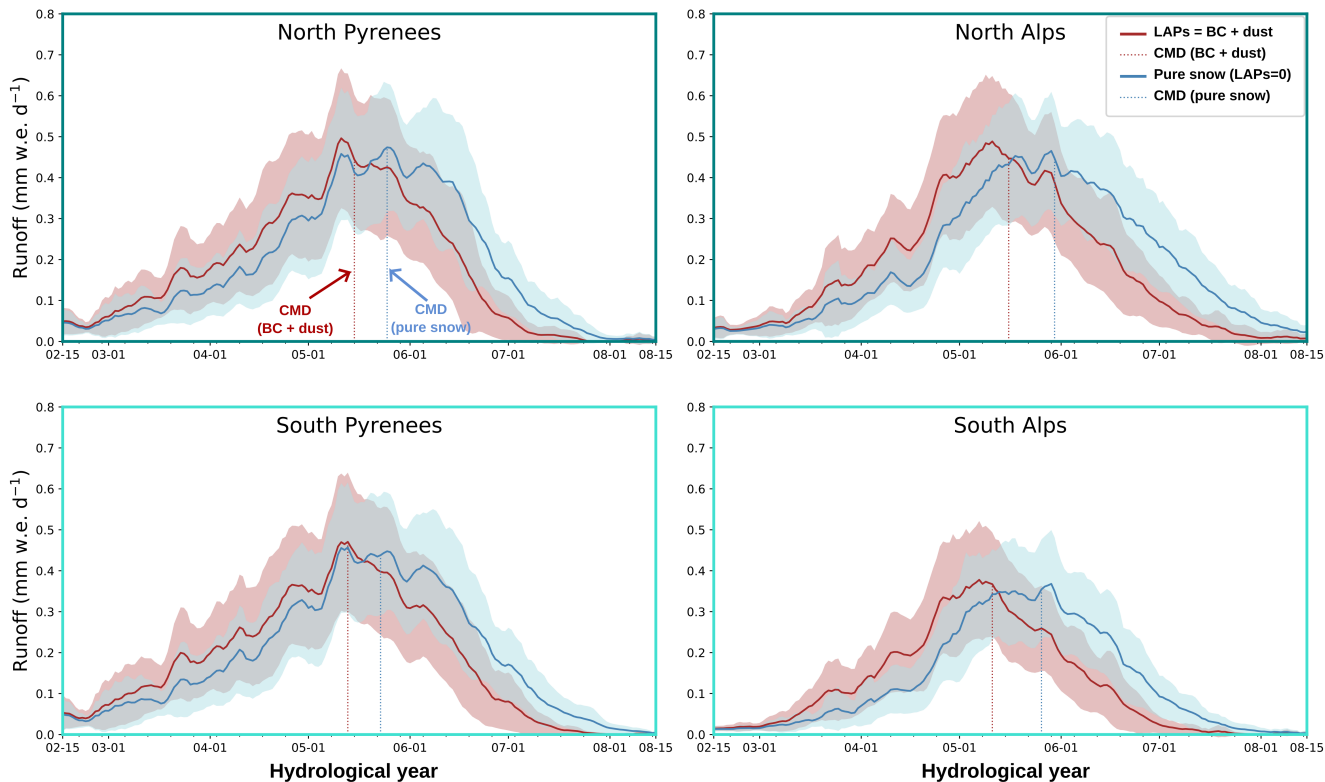


**Fig. 4: Runoff from snowmelt averaged over the period 1979–2018 (solid line) with the standard deviation (shaded areas) representing the annual variability. Pure simulations are represented in blue and simulations considering the effect of BC and dust are in red. The center of mass date of each simulation, defined as the date for which half of the total annual runoff from snowmelt is reached, are indicated by the dashed lines.**

## Supplementary Files

This is a list of supplementary files associated with this preprint. Click to download.

- [ReveilletetalNCommSuppMat.pdf](#)